Universiteit
Leiden
The Netherlands

Crossing barriers, delivery of llama antibody fragments into the brain

Rotman, M.

Citation
Rotman, M. (2017, April 19). *Crossing barriers, delivery of llama antibody fragments into the brain*. Retrieved from https://hdl.handle.net/1887/48860

Version:	Not Applicable (or Unknown)
License:	Licence agreement concerning inclusion of doctoral thesis in the Institutional Repository of the University of Leiden
Downloaded from:	https://hdl.handle.net/1887/48860

Note: To cite this publication please use the final published version (if applicable).

Cover Page

Universiteit Leiden

The handle http://hdl.handle.net/1887/48860 holds various files of this Leiden University dissertation

Author: Rotman, M.
Title: Crossing barriers, delivery of llama antibody fragments into the brain
Issue Date: 2017-04-19

2

CHAPTER

VHH AGAINST BACE1 INHIBITS BETA-SECRETASE ACTIVITY *IN VITRO* AND *IN VIVO*

Adapted from

Camelid heavy chain only antibody fragment domain against β-site of amyloid precursor protein cleaving enzyme 1 inhibits β-secretase activity in vitro and in vivo.

Bram Dorresteijn [1], Maarten Rotman [2,3], Dorien Faber [1], Ruud Schravensande [1], Ernst Suidgeest [3], Louise van der Weerd [2,3], Silvère M. van der Maarel [2], Theo C. Verrips [1] and Mohamed el Khattabi [1].
FEBS Journal **282** (2015) 3618-3631

ABSTRACT

Introduction: Accumulation and aggregation of the amyloid-beta (Aβ) peptide is associated with Alzheimer's disease (AD). Aβ is generated from the amyloid precursor protein by the successive action of two membrane-associated processing enzymes: β-secretase or β-site of amyloid precursor protein cleaving enzyme 1 (BACE1) and γ-secretase. Inhibition of one or both of these enzymes prevents Aβ generation and the accompanying Aβ accumulation. Antigen binding fragments from camelid heavy chain only antibodies (VHHs) were found to exert excellent enzyme inhibition activity.

Methods: In the present study, we generated VHHs against BACE1 by active immunization of *Lama glama* with the recombinant BACE1 protein. Two classes of VHHs were selected from a VHH-phage display library by competitive elution with a peptide encoding the Swedish mutation variant of the BACE1 processing site.

Results: One VHH was found to inhibit the enzyme activity of BACE1 *in vitro* and in cell culture, whereas two other VHHs were found to stimulate BACE1 activity under the same conditions *in vitro*. Furthermore, an *in vivo* study with a transgenic AD mouse model, using intracisternal injection of the inhibitory VHH, led to acute reduction of the Aβ load in the blood and brain.

Conclusion: This inhibitory VHH may be considered as a candidate molecule for a therapy directed towards reduction of Aβ load and prevention of AD progression. Both the inhibitory and stimulatory VHH may be useful for improving our understanding of the structure-function relationship of BACE1, as well as its role in AD progression.

1. INTRODUCTION

Alzheimer's disease (AD) is a devastating neurodegenerative disease and the most common form of dementia [1]. AD is characterized pathologically by the presence of extracellular senile plaques and intracellular degeneration, including neurofibrillary tangles, dystrophic neuritis and neuropil threads [2]. The major constituent of senile plaques is amyloid-beta (Aβ), a small 4-kDa peptide. Aβ is the result of the proteolytic processing of a larger membrane bound precursor protein named amyloid precursor protein (APP). Processing of APP starts with the cleavage of APP by β-secretase, also named β-site of APP cleaving enzyme (BACE1), which generates an extracellular soluble APPβ fragments and a membrane bound C-terminal fragment (CTFβ or C99) [3]. Subsequently, C99 is cleaved by γ-secretase into Aβ peptides of predominantly 40 and 42 amino acids long (Aβ40 and Aβ42) on one side and a small membrane bound peptide (AICD) on the other [4]. This proteolytic processing is known as the pathologic processing pathway or amyloidogenic pathway. An alternative processing pathway initiated by α-secretase prevents the generation of CTFβ, as the α-secretase cleaves APP within the Aβ region and generates a soluble extracellular APPα and a C-terminal fragment (CTFα or C83). After subsequent cleavage of CTFα with γ-secretase, a small peptide (P3) is generated. This P3 peptide does not have any known pathological effects and its function is unknown [5]. This alternative processing pathway is known as the non-pathological pathway or non-amyloidogenic pathway.

BACE1, also known as Asp2 [6] and Memapsin2 [7], is a 501 amino acid long transmembrane aspartic protease. A total of four different splice variants can be transcribed from the BACE1 locus, of which the most active isoform is predominantly found in the brain [8]. β-secretase activity is solely dependent of BACE1 protein [6,7,9–11], whereas γ-secretase is a complex of many proteins, including presenilin, nicastrin, anterior pharynx-defective 1 and presenilin enhancer 2 [12].

In AD patients, both expression levels and activity of BACE1 are found to be increased [13,14]. Furthermore, the highest levels of BACE1 are found at sites close to amyloid plaque deposits [14–16]. Involvement of BACE1 in AD pathology was confirmed in transgenic mice *in vivo*. Cross-breeding transgenic mice overexpressing human APP with BACE1-null mice abolishes Aβ production and Aβ plaque formation [17,18], even in the brains of old mice [19]. Because embryonic knockdown of BACE1 is well tolerated [20], and an absence of BACE1 activity abolished the Aβ load, it is expected that inhibition of BACE1 may stop AD progression without any major side effects. Therefore, several BACE1 inhibitor candidates, *e.g.* TAK-070, TC-1, AZ-4217, have been developed, of which 10 candidates are currently investigated in clinical trials [21–26]. Moreover, and relevant for a highly selective therapy, BACE1 activity was found to be susceptible to antibody-mediated inhibition [27,28]. Active immunization of transgenic

AD mice (Tg2576) with BACE1 [29], as well as treatment with BACE1 inhibitory antibodies [27], reduce Aβ load and block APP processing.

Despite all efforts, no BACE1 inhibitor has been approved for therapy so far. Therefore, new approaches to develop BACE1 inhibitors are needed. Both small molecule inhibitors and conventional antibodies have benefits, as well as disadvantages. With antibodies, great specificity can be achieved by careful selection, resulting in less possible side effects upon administration. Next to that, a more homogenous maintained level of therapeutic molecules is generally achieved among patients, as well as the possibility of a more patient-friendly administration regime (lesser dosing), compared to small molecule inhibitors [26,30]. A special class of antibodies, found in *Camelidae*, could be utilized to develop an alternative candidate belonging to the antibody approach. The antibody repertoire of *Camelidae* (*Lama glama, Vicunga pacos, Camelus bactrianus* and *Camelus dromedaries*) consists of two classes of the IgG family. Next to conventional IgG made by the combination of heavy and light chain dimers, another IgG class devoid of light chains was discovered in the early 1990's [31]. The isolated variable domain of this heavy chain only IgG (camelid heavy chain only antibody fragment; VHH) was found to be fully functional and therefore the smallest known naturally derived antigen-binding fragment. VHHs show a number of advantages over conventional IgGs and IgG derivatives such as Fabs or scFv. Among those advantages are easy production [30], inhibition of enzymatic activity by proteolytic cleft entry [32], and possible passage though the blood-brain barrier (BBB) [33,34].

The present study aimed to develop BACE1-targeting VHHs for passive immune therapy of AD. We describe the generation of BACE1 VHH-immune libraries, *in vitro* selection of VHHs that bind BACE1 and the characterization of VHHs that inhibit or stimulate the enzymatic activity of BACE1. VHHs exerted their inhibition or stimulation of BACE1 *in vitro* using purified BACE1 protein. The *in vitro* inhibition was validated in a cellular assay, using mouse neuroblastoma cells (N2a), which express BACE1 and which were transfected with the human APP gene harboring the Swedish mutation (N2a-APP_{swe}) [35]. The inhibitory VHH (VHH-B3a) showed a significant effect on the activity of BACE1 in the cell assay when measured using a fluorogenic peptide as a BACE1-specific substrate. Furthermore, the effect of the inhibitory VHH was validated in an *in vivo* experiment. A bolus dose of VHH-B3a injected into the cisterna magna of double transgenic mice, overexpressing both human APP with the Swedish mutation and human presenilin 1 with exon 9 deletion (APP_{swe}/PS1dE9) reduced Aβ concentration in both plasma and brain.

2. MATERIALS AND METHODS

2.1. Immunization and library construction

The immunizations were approved by the Utrecht University institutional Animal Experiments Committee (DEC permit: 2007.III.01.013). Two llamas were immunized with 50 μg of purified BACE1 (product number 931-AS; R&D systems, USA) in 1 ml of PBS mixed with the adjuvant Stimune (Prionics, NL) and injected intramuscularly. The immunization scheme consisted of a priming immunization (at day 0), followed by three boosts (at days 14, 28 and 35).

The immune response was measured in the immune sera taken at days 28 and 43 and were compared with the pre-immune serum taken at day 0. BACE1 (100 ng) in PBS was coated into wells of a 96-wells Maxisorb plate (Nunc, USA) overnight at 4°C. After blocking with 4% skimmed milk (Marvel; Premier Foods, UK) in PBS (mPBS), serial dilutions of the immune and pre-immune sera were added to the wells. A heavy chain only IgG response was detected with a rabbit polyclonal serum directed against VHH (RaVHH; in-house made) and a secondary donkey anti-rabbit antibody coupled to horseradish peroxidase (DaRPO; Invitrogen, USA). Peroxidase activity was measured using orthophenylenediamine (OPD) + H_2O_2, and A_{490} via a spectrophotometer (Bio-Rad, USA).

At day 43, peripheral blood lymphocytes were purified from 150 ml of blood on a Ficoll gradient (GE Healthcare, UK). RNA was isolated from these peripheral blood lymphocytes and converted into cDNA using SuperscriptIII kit (Invitrogen). IgG binding domains were amplified via PCR using primers annealing at the signal sequence of the IgGs and the hinge region [36]. The approximately 700-bp fragments corresponding to the antigen binding domain of the heavy chain only antibodies (VHH) were excised from gel, and the *Sfi*I restriction site was introduced at the 5' end by a nested PCR step to facilitate cloning into the display vector. The purified 700-bp fragment was digested with *Bst*EII (a restriction site found in the hinge region of heavy chain only antibodies) and *Sfi*I (Fermentas, USA). The resulting approximately 400-bp antigen binding fragment of the heavy chain only antibodies was cloned in a phage-display plasmid. The plasmids were transferred to *Escherichia coli* strain TG1 [*supE hsd_5 thi* (*lac-proAB*) F_(*traD36 proAB_lacI*q *lacZ_M15*)] by electroporation. *E. coli* TG1 was used for the production of phages, the infection by selected phages, and for expression of selected VHH.

2.2. Selection and screening of anti-BACE1 VHH

Phage display [37] was used to select phages that specifically bind recombinant BACE1 (931-AS; R&D systems). Maxisorp 96-wells plates (Nunc) were coated overnight at 4°C with 2, 10 or 50 μg/ml BACE1 in PBS. The next day, wells were blocked with 4% mPBS. Subsequently, phages

produced from the BACE1 immune VHH-phage library were pre-incubated in 2% mPBS and added to the wells containing BACE1. As a control, phages were added to non-coated, blocked wells. Phages were incubated for 2 h at room temperature (RT). After extensive washing with PBS containing 0.05% Tween-20 (PBST; Sigma-Aldrich, USA) and with PBS, bound phages were eluted with 100 mM triethylamine (TEA; Sigma-Aldrich) by 15 min. incubation at RT. Eluted phages were directly neutralized by the addition of 1 M Tris-HCl (pH 7.5). These output phages were used to infect exponentially growing *E. coli* TG1 cells. Infected cells were plated on LB agar plates containing 2% glucose and 100 μg/ml ampicillin. For the production of phages, *E. coli* containing phagemids were infected with helper phage VCSM13, and phage particles were produced overnight at 37°C in medium supplemented with 100 μg/ml ampicillin and 25 μg/ml kanamycin. After purification, phages were used for a second round of panning selection against recombinant BACE1 as described above. However, bound phages were now selectively eluted by incubation with either peptide APP_{swe} (EEISEVNLDAE) or APPwt (EEISEVKMDAE) for various time periods. The peptides represented the BACE1 processing site in APP with and without the Swedish mutation, respectively (mutation sites underlined) [38]. Peptides were synthesized at the department of Membrane Enzymology (Utrecht University, NL).

For screening, single clones were grown into 96-wells plates and phage production was induced by infection with helper phage and selection for kanamycin and ampicillin resistance. Phages were separated from bacteria by centrifugation. BACE1 (2 μg/ml) was coated overnight onto Maxisorp 96-wells plates (Nunc) and the purified phages were incubated on the coated plates at RT for 2 h. After extensive washing with PBST and PBS, bound phages were detected using an anti-M13 antibody conjugated to horseradish peroxidase (GE Healthcare) and OPD. Twelve independent clones that showed high ELISA signals were selected for sequencing (ServiceXS, NL) and further characterization.

For production of VHH proteins, selected VHHs were subcloned into an expression plasmid. The 400-bp *Sfi*I-*Bst*EII fragments were excised from the selected plasmids and cloned into the expression plasmid pMEK222 (present study), using the same restriction sites. VHHs expressed from pMEK222 are fused to carboxyterminal FLAG and hexa-histidine tags.

2.3. Production and purification of anti-BACE1 VHH

VHHs were expressed from the plasmid pMEK222 by inducing a 400 ml log-phase *E. coli* culture with 1 mM IPTG (Fermentas) and incubation for 5 h at 37°C. The bacteria were harvested by centrifugation (15 min. at 4566 × g) and frozen overnight at -20°C. After thawing the bacteria and resuspending them in 20 ml of sonication buffer (50 mM sodium phosphate, 300 mM NaCl, pH 7.0), periplasmic fractions were prepared by incubating the resuspended bacteria head-over-head for 1 h at RT, and separating periplasmic soluble fractions, containing the

VHHs, from cellular debris by 15 min. of centrifugation at 4566 × g. VHHs were purified from the soluble periplasmic fractions via the hexa-histidine tag using Talon beads (product number 635504; Clontech, USA). Talon beads were incubated with the periplasmic fraction for 1 h at RT. After several washings with PBS (or sonication buffer), bound VHHs were eluted with 300 mM imidazole in sonication buffer. Fractions containing purified VHH were subsequently pooled and dialyzed overnight at 4°C against PBS.

2.4. Characterization of anti-BACE1 VHH

Purified VHHs were evaluated for binding of immobilized BACE1. Maxisorp 96-wells plates (Nunc) were incubated with 1 μg/ml BACE1 overnight at 4°C. Subsequently, serial dilutions of VHHs in 2% mPBS were added and incubated while shaking for 2 h at RT. The wells were washed three times with PBST and once with PBS before the addition of 100 μl of RaVHH (1:2000; in-house made) in 1% mPBS to detect VHHs. After washing the wells as before, DaRPO (1:10000; Invitrogen) in 1% mPBS was used as secondary antibody. OPD and H_2O_2 were used as before to visualize VHH binding. K_d values for VHH were calculated using GraphPad Prism version 5.01 for Windows (GraphPad Software, USA) using a one site-specific binding curve.

2.5. Cell culture

Mouse N2a neuroblastoma cells stably transfected with APP_{swe} (N2a-APP_{swe}) were kindly provided by Dr. B. Kleizen (Department of Chemistry, Faculty of Science, Utrecht University). N2a-APP_{swe} were cultured at 37 °C and 5% CO_2 in medium made up by 47.5% DMEM (Gibco, USA), 47.5% OptiMEM reduced serum medium (Gibco), 5% Fetal Bovine Serum (FBS; Gibco), 300 μg/ml L-Glutamine, 100 μg/ml penicillin, 100 μg/ml streptomycin, and 200 μg/ml geneticin (Invitrogen)

2.6. BACE1 activity assay

BACE1 activity was measured using the fluorogenic peptide MCA-[SEVNLDAEFRK](Dnp)RR (R&D Systems). A highly fluorescent 7-methoxycoumarin group (MCA) was combined with a peptide containing the BACE1 processing sequence of APP_{swe}. This fluorophore-peptide combination was connected to a 2,4-dinitrophenyl group (Dnp), which functions as a quencher of MCA. After digestion of the peptide by BACE1, the fluorescent group and the quencher will be separated and fluorescence can be measured. In this assay, the amount of fluorescence is proportional to BACE1 activity.

Purified BACE1 (~35 nM) was incubated with 10 nM MCA-[SEVNLDAEFRK](Dnp)RR in sodium acetate buffer, pH 5.5 at 37°C for 2 h. MCA fluorescence was measured every 2 min. using FluoSTAR Optima (320 nm excitation, 405 nm emission; BMG Labtech, DE) for the entire 2 h.

The effect of VHH on the activity of the BACE1 enzyme was assayed by the addition of various concentrations VHH (between 10 nM to 20 μM) to the mixture at the beginning of the 2 h incubation and measurement time. The effect was compared to the effect of 5 nM of BACE1-Inhibitor-IV (Calbiochem, USA), which inhibits the activity of the enzyme completely. GraphPad Prism v5.01 was used to determine slopes of activity as described for the recombinant BACE1 activity assay, as well as for the statistical analysis.

The effect of VHH-B3a on BACE1 activity was also measured by determining the concentration of produced Aβ40. Fresh medium or medium containing 10 μM VHH-B3a was added to cultured N2a-APP_{swe} cells. After 1, 5 and 24 h, Aβ40 concentration was determined in undiluted cell culture medium using a commercial ELISA kit (product number KHB3482; Invitrogen) in accordance with the manufacturer's instructions. The determined Aβ40 concentration of untreated cell medium was set at 100% for each time point and was related to the Aβ40 concentration of the treated cell medium.

2.7. Animal studies

The *in vivo* study to determine the therapeutic value of the BACE1-inhibiting VHH-B3a was performed in 4-5 months old female transgenic mice or female wildtype littermates from a colony set up using the APP_{swe}/PS1dE9 strain (APP/PS1; JAX® Mice and Services, The Jackson Laboratory, USA). The animal study was carried out in compliance with the Dutch laws related to the conduct of animal experiments and approved by the institutional Animal Experiments Committee (DEC permit 11133) of the Leiden University Medical Center.

2.8. VHH biodistribution

VHH were labelled with an infrared dye (IRD800CW; LiCor, USA) to image VHH distribution throughout the brain. VHH-B3a was incubated for 2 h. at RT while tumbling with NHS-IRD800CW (LiCor). Subsequently, uncoupled IRD800CW was removed with a Zeba Desalting spin column (Invitrogen) in accordance with the manufacturer's instructions. Coupling of NHS-IRD800CW was validated by gel electrophoresis and the concentration was determined using a spectrophotometer (NanoDrop, USA). Activity of VHH-B3a-IRD800CW (B3a-IRD800) was measured as described with recombinant BACE1 and compared with non-conjugated VHH-B3a.

The mouse heads were shaved before 75 μg of B3a-IRD800 was administered via a percutaneous intracisternal bolus injection in wildtype mice (n = 4) to evaluate the efficacy of the injection procedure and the distribution of VHH over the brain [39]. *In vivo* fluorescence was determined at six time points (0, 1, 3, 6, 24, and 48 h) in the same mice. Mice were anaesthetized using continuous 1-2% isoflurane inhalation gas and dorsal images were taken using a LiCor

Pearl Impulse Imager (LiCor). Acquired *in vivo* images were quantified with LiCor software, by assigning a region of interest and determining fluorescence intensity. At 6, 24, and 48 h, directly after imaging, one mouse was sacrificed by perfusion-fixation (PBS and 4% PFA) under deep anaesthesia from pentobarbital (Euthasol; NL). Post-mortem fluorescence imaging was performed on the intact brain to confirm the VHH distribution. Brains were sectioned in 1 mm thick slices and imaged using LiCor Odyssey imager to visualize the B3a-IRD800 distribution throughout the brain. Intracisternal injection failed in one mouse. This mouse was excluded from the VHH biodistribution determination.

2.9. In vivo therapy

A bolus of 75 µg B3a-IRD800 was administered intracisternally in transgenic mice (n = 5) as described above. A control group (n = 5) was injected with PBS. Wildtype mice received the same treatment (n = 5 for both groups). Blood samples were collected just before injection and at 6, 24, and 48 h after injection. Blood samples were immediately centrifuged for 10 min. at 3000 × g. Plasma was separated from the cellular component and aliquots were stored at -80°C until use. Mice were sacrificed after 48 h by perfusion-fixation as described above. After fixation, brains were separated into left and right hemispheres. The right hemisphere was frozen in isobutanol on dry ice and stored at -80°C. The left hemisphere was further fixed in either 4% PFA or 2% PFA with 0.2% glutaraldehyde for 3 h at RT followed by 24 h of incubation at 4°C. Subsequently, fixative solutions were replaced for all brains by 2% PFA and brains were stored at 4°C. The right hemisphere was weighed, homogenized with an ultrathorax in extraction buffer (25 mM Tris-HCl, pH 7.6, 150 mM sodium chloride, and Complete Protease Inhibitor Cocktail; Roche Diagnostics, CH), and then sonicated with an M-150 sonicator. For analysis of the soluble Aβ fraction, brain homogenates were centrifuged at 100 000 × g for 1 h at 4°C. Supernatants were used to determine soluble Aβ. The concentrations of Aβ40 in both plasma and brain samples were determined with a commercial ELISA kit (product number KHB3482; Invitrogen). The concentrations of Aβ42 were determined only in the plasma samples (ELISA, product number KHB3544, Invitrogen). Because of technical difficulties, the reported value of Aβ42 concentration in plasma at 6 h consists of samples from two mice, all other reported Aβ40 and Aβ42 values are derived from samples from all five mice. Despite careful treatment, minor differences in, for example, transport and storage influences the measured absolute Aβ concentration [40,41]. To exclude any difference in absolute Aβ as a result of treatment per time point, Aβ concentrations are plotted against the control at that time point.

The wet weight of the brain was used to calculate the density of soluble Aβ40 in the brain (pmol/g). Both Aβ40 and Aβ42 concentrations in plasma were calculated and expressed as the

Aβ concentration (pM). GraphPad Prism v5.01 was used to perform statistics on differences between treated and untreated groups.

2.10. Statistical analysis

GraphPad Prism v5.01 was used to determine the slope of the BACE1 activity curves of each VHH concentration by linear regression. IC_{50} and EC_{50} of BACE1 inhibition or activity was calculated by nonlinear fitting log(inhibitor/agonist) versus response and variable response. A Student's *t*-test to evaluate differences between two groups and an analysis of variance (ANOVA) with Tukey's post-hoc test to evaluate differences between more than two groups were performed with $p<0.05$ considered statistically significant.

3. RESULTS

3.1. Selection of BACE1 VHH

VHHs binding specifically to BACE1 were selected using phage display from an immune library obtained from llama immunized with BACE1. Two rounds of panning selection were applied. In the first round, phages binding to BACE1 were eluted by pH shock. These phages were used as input for a second round of selection, in which bound phages were eluted selectively by competition with a peptide containing the recognition sequence of BACE1 on the APP_{swe} mutation (KM670/671NL). Monoclonal phages were further characterized using binding to immobilized BACE1 and immune detection. This resulted in the selection of 28 different clones.

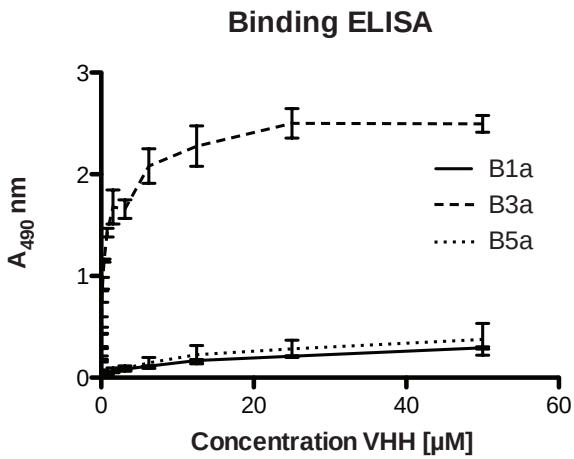

Figure 2.1. VHH binding to BACE1. BACE1 (100 ng) was immobilized onto a Nunc 96-well Maxisorb plate and incubated with serial dilutions of the indicated VHH. Bound VHHs were detected with rabbit anti-VHH and donkey anti-rabbit coupled to horseradish peroxidase.

Table 2.1. Binding affinities of anti-BACE1 VHH. VHHs were titrated and allowed to bind immobilized BACE1 in an ELISA. Affinity calculations were performed with a 'one site specific binding curve' algorithm (GrapPad Prism v5.01).

VHH	K_d (μM)
B1a	10.8 ± 1.33
B3a	0.3 ± 0.03
B5a	9.3 ± 1.67

The VHHs from these clones were produced and purified, and then tested for binding to immobilized BACE1 and immune detection. This second round of characterization resulted in 12 VHHs, which displayed a 175% higher signal by ELISA compared to non-coated control wells. Sequencing of these 12 independent clones revealed three different sequences, represented by VHH-B1a, -B3a, and -B5a. Figure 2.1 shows a typical dose-response curve for the VHHs binding to immobilized BACE1. The values were used for the calculation of the K_d values (Table 2.1). VHH-B1a and VHH-B5a have low affinity to immobilized BACE1 (K_d = ~ 10 μM), whereas VHH-B3a has an affinity that is ~ 33-fold higher (K_d = ~ 0.3 μM).

3.2. Inhibition of recombinant BACE1 by VHH

The effect of VHH on recombinant BACE1 activity, either inhibitory or stimulatory, was evaluated using a reporter substrate that consists of a fluorescent group connected to a quencher. Figure 2.2 shows representative fluorescent signals recorded during a triplicate experiment of a single concentration of VHH-B1a (20 μM) with BACE1 (35 nM) and a BACE1 (35 nM) without VHH as control. The slope reflects the relative BACE1 activity, with lower values indicating more efficient inhibition. The addition of 20 μM VHH-B1a increased BACE1 activity by 400% and 20 μM VHH-B5a increased the activity by 200% (Figure 2.3 A and C). However, the addi-

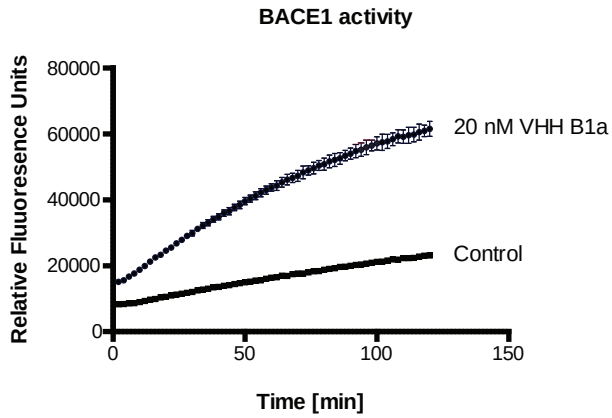

Figure 2.2. Stimulation of BACE1 activity by VHH-B1a. Recombinant BACE1 (~ 35 nM) was incubated alone or with 20 μM VHH-B1a, and enzymatic activity was assayed using MCA-[SEVNLDAEFRK](Dnp)RR. Fluorescent MCA, separated from the Dnp quencher after cleavage of the substrate by BACE1, was measured of 2 h with FluoSTAR. BACE1 without any additions (Control) was used as positive control. Best fit linear was calculated to determine slope (RFU/Δ*t*).

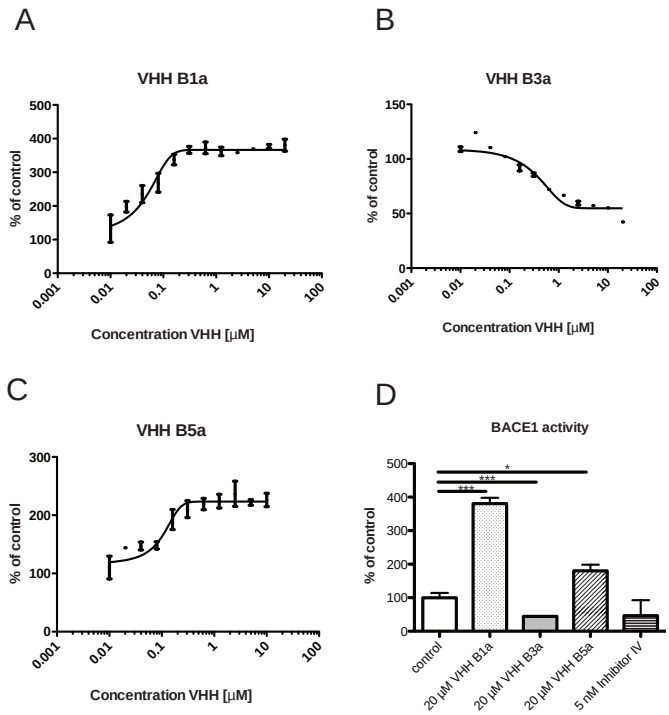

Figure 2.3. Effect of the selected VHH on BACE1 enzyme activity. Recombinant BACE1 (~ 35 nM) was incubated with serial dilutions of VHH-B1a (A), VHH-B3a (B) and VHH-B5a (C). Enzymatic activity was assayed using MCA-[SEVNLDAEFRK](Dnp)RR. Fluorescent MCA, separated from the Dnp quencher after cleavage of the substrate by BACE1, was measured with FluoSTAR. As a control for the inhibition of BACE1 activity, 5 nM Inhibitor IV was used (D). Data represent the relative BACE1 activity compared to control with the SEM indicated. VHH-B1a and -B5a show BACE1 activity increase (relative $logEC_{50}$ ~ 0.3 μM and $logEC_{50}$ ~ 0.1 μM, respectively) while VHH-B3a shows inhibition of activity (relative $logIC_{50}$ ~ 0.9 μM). One-way ANOVA was performed. * = $p < 0.05$, *** = $p < 0.0005$.

tion of 20 μM VHH-B3a to BACE1 was found to decrease BACE1 activity by 50% compared to control (Figure 2.3 B). The inhibition of BACE1 activity by VHH-B3a is equal to the effect of 5 nM Inhibitor IV (Figure 2.3 D).

VHH-B1a and -B3a were subsequently tested in an N2a-APP_{swe} cellular assay. The two VHHs and the reporter peptide were incubated with the cells for 2 h. Figure 2.4 shows the relative increase of fluorescence signal recorded during 2 h. VHH-B3a was found to decrease BACE1 activity (Figure 2.4 B). An inhibition of BACE1 activity of 50% was reached with 6.5 μM VHH, which is comparable to the inhibition of purified BACE1 *in vitro* at an equal concentration. By contrast to the *in vitro* results, VHH-B1a had only minor effect on the cellular BACE1 activity (Figure 2.4 A). Similar to the *in vitro* results, VHH-B3a inhibits BACE1 activity in the cellular assay equally compared to 5 nM Inhibitor IV (Figure 2.4 C).

The observed decrease in activity was validated by the detection of Aβ40 concentration in the

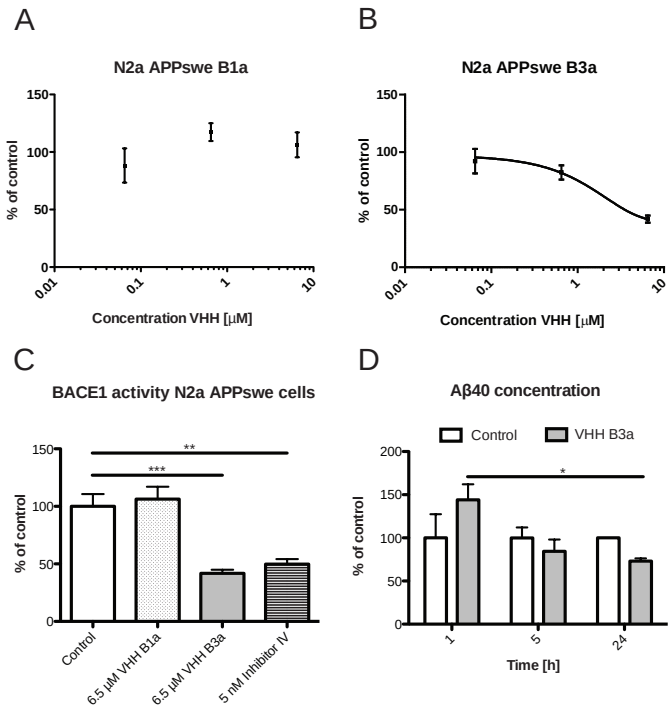

Figure 2.4. Inhibition of cellular BACE1 by VHH-B3a. N2a-APP$_{swe}$ cells incubated with serial dilutions of VHH-B1a **(A)** and VHH-B3a **(B)** and enzymatic activity was assayed using MCA-[SEVNLDAEFRK](Dnp)RR. Fluorescent MCA, separated from the Dnp quencher after cleavage of the substrate by BACE1, was measured with FluoSTAR. VHH-B3a shows BACE1 activity inhibition activity (relative logIC_{50} ~ 0.9 μM), whereas for VHH-B1a no relative logEC_{50} could be calculated. As a control for the inhibition of BACE1 activity, 5 nM Inhibitor IV was used **(C)**. Data represent the relative BACE1 activity compared to control with the SEM indicated. One-way ANOVA was performed. * = $p < 0.05$, ** = $p<0.005$, *** = $p < 0.0005$. Aβ40 produced by N2a-APP$_{swe}$ cells treated with VHH-B3a was quantified using an ELISA and compared with untreated cells **(D)**. Data represent duplicate experiments, except t = 24 h in the control situation, which is a single experiment. One-way ANOVA showed a significant difference between 1 and 24 h treatment ($p < 0.05$)

supernatant of N2a-APP$_{swe}$ cells. Fresh medium containing a 10 μM concentration of VHH-B3a was added to the cells and aliquots of the medium were sampled over time. After treatment of the cells for 5 h with VHH-B3a, a reduction in Aβ40 amount was measured. At 24 h this reduction was significant compared to the concentration obtained from the medium of control cells (Figure 2.4 D).

3.3. In vivo imaging of VHH-B3a

For *in vivo* analysis of the BACE1-specific VHH-B3a, we delivered the VHH directly into the *cisterna magna* using an intracisternal injection. To be able to image the distribution of the VHH from the *cisterna* over the brain, VHH-B3a was randomly labelled with the near infrared dye IRD800, as confirmed by SDS gel electrophoresis (Figure 2.5 A). Inhibition of BACE1 activity by VHH-B3a-IRD800 was measured to assess whether the labelled VHH was still functional. The

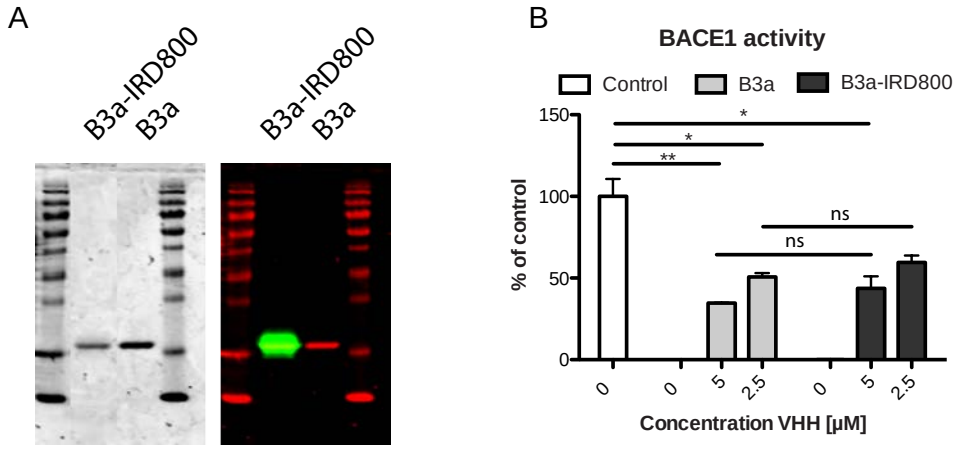

Figure 2.5. Labeling of VHH-B3a with NHS-IRD800CW. VHH-B3a was coupled to NHS-IRD800CW, analyzed by SDS-PAGE and imaged with a LiCor Odyssey Imager **(A)**. Inhibition of BACE1 activity by IRD800 labeled VHH-B3a was compared to non-labeled VHH-B3a. No significant (ns) difference between equal concentrations of IRD800 labeled and non-labeled VHH-B3a was observed **(B)**. One-way ANOVA was performed. * = $p < 0.05$, ** = $p<0.005$.

inhibitory effect was still present, and only slightly reduced by 10% compared to non-labelled VHH-B3a (Figure 2.5 B).

Intracisternal injections of VHH-B3a-IRD800 resulted in a clear distribution of the labelled VHH over the entire mouse brain (Figure 2.6). With complete distribution throughout the brain, a theoretical concentration of 1 μM VHH in brain tissue could be expected. Two mice showed a similar accumulation and distribution of VHH-B3a-IRD800 throughout the brain (Figure 2.6 A, mouse 1 and mouse 2), whereas the control mice, injected with PBS, did not show any signal (Figure 2.6 A, mouse 3). With increasing time after injection, the amount of VHH-B3a-IRD800 gradually decreased, likely as a result of brain clearance (Table 2.2). Subsequently, 1 mm thick slices of the brains of all three mice were imaged to visualize the distribution of VHH-B3a-IRD800 throughout the brain (Figure 2.6 B). These brain slices demonstrate a homogeneous distribution of the VHH through the entire brain, indicating that intracisternal

Table 2.2. *In vivo* quantification of injected VHH-B3a-IRD800. A bolus injection of VHH-B3a-IRD800 was administered intracisternally into wildtype mice. At six time points after injection *in vivo* images were acquired and quantified. Values are expressed as the mean IRD800 signal in the Region of Interest (mean ± SEM).

Time after injection (h)	Mouse 1	Mouse 2	Mouse 3
0	$3.40 \pm 1.12 \times 10^4$	$4.14 \pm 0.31 \times 10^3$	$3.78 \pm 4.60 \times 10^{-4}$
1	$2.76 \pm 1.15 \times 10^4$	$6.48 \pm 0.48 \times 10^3$	$4.49 \pm 4.87 \times 10^{-4}$
3	$1.56 \pm 0.62 \times 10^4$	$6.31 \pm 0.47 \times 10^3$	$7.84 \pm 5.33 \times 10^{-4}$
6	$1.90 \pm 0.57 \times 10^4$	$5.80 \pm 0.43 \times 10^3$	$8.26 \pm 8.26 \times 10^{-4}$
24		$1.87 \pm 0.43 \times 10^3$	$3.87 \pm 3.87 \times 10^{-4}$
48			$2.47 \pm 2.47 \times 10^{-4}$

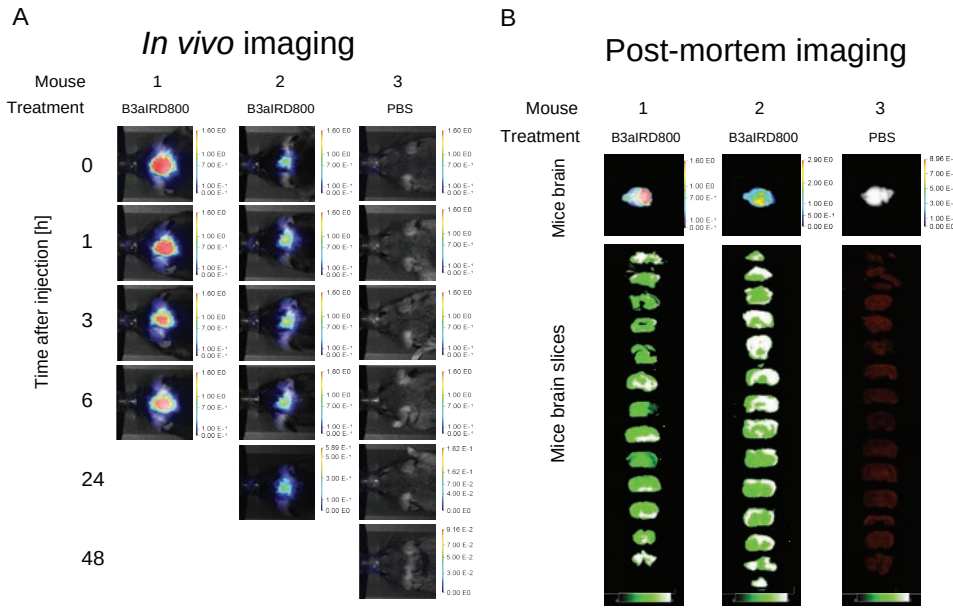

Figure 2.6. Cranial distribution of IRD800 labeled VHH-B3a injected in *cisterna magna*. Three wildtype mice were successfully injected intracisternally with a bolus of 75 µg of VHH-B3a-IRD800 (1-2) or PBS (3) and dorsally imaged *in vivo* at the indicated time points **(A)**. Mice were sacrificed at different time points after injection (6, 24 and 48 h, respectively) by perfusion-fixation with PBS and 4% PFA. Fixed brains were imaged from the dorsal side **(B)**. Entire fixed brains were cut in 1 mm thick slices and imaged to visualize the distribution of VHH-B3a-IRD800 (same mouse indication).

injection can be used to deliver VHH-B3a-IRD800 into the brains of mice for an *in vivo* BACE1 inhibition assay.

3.4. In vivo BACE1 inhibition

To assess *in vivo* BACE1 inhibition, we injected a bolus of 75 µg of VHH-IRD800 intracisternally into APP_{swe}/PS1dE9 double transgenic mice and wildtype littermates. A bolus of PBS was injected in equally sized groups as untreated controls. Concentration of both Aβ40 and Aβ42 in plasma, as well as the concentration of Aβ40 in whole brain homogenates were measured (Figure 2.7).

Prior to injection, blood samples were taken to determine the plasma levels of Aβ40 and Aβ42 in the transgenic mice for both the VHH treated group and the control group, to exclude group specific differences in Aβ concentration. To evaluate plasma concentrations over time, the concentration of the control group is set 100% for each time point and compared with VHH-B3a-IRD800. Concentrations of Aβ40 in plasma were equal prior to treatment (Figure 2.7 A) but Aβ42 plasma concentrations differed slightly, though not significantly, between the treated and untreated groups (Figure 2.7 B). At different time points after injection, we observed an almost significant decline in Aβ40 concentration (Figure 2.7 A). The largest

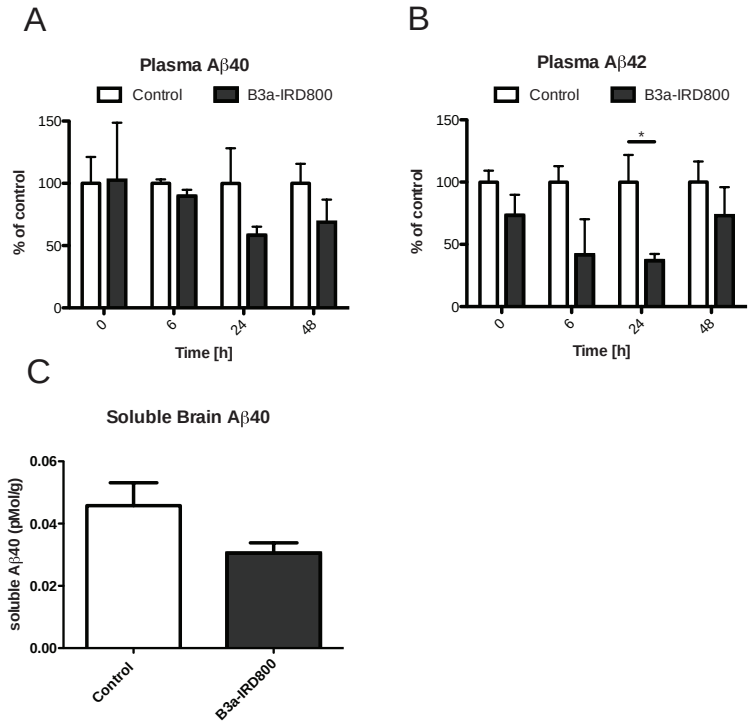

Figure 2.7. *In vivo* BACE1 inhibition by VHH-B3a-IRD800. Aβ concentrations in plasma of double transgenic APP_{swe}/PS1dE9 mice were measured before and after injection of VHH-B3a-IRD800 (n = 5) or PBS (n = 5) at the indicated time points. Plasma concentrations of the PBS control group are set at 100% for each time point. An equal plasma concentration of both Aβ40 and Aβ42 was measured before injection between the VHH treated and the control group. An almost significant difference in plasma Aβ40 concentration was observed after 24 h **(A)**. For the Aβ42 plasma concentration the difference after 24 h was clearly significant (* = $p < 0.05$; **B**). The reduction of soluble Aβ40 in homogenized brain extracts showed a decreased density of Aβ40 in the treated group compared to the control (C). Bars represent the average concentration per treatment. The SEM is indicated. Student's *t*-test analysis was performed.

decline in Aβ40 plasma concentrations is reached at 24 h after injection. At 48 h after injection, the decline in plasma concentration appears to be less apparent compared to 24 h after injection. A similar pattern is observed for the concentration of Aβ42 in plasma (Figure 2.7 B). A significant decrease of Aβ42 plasma concentration was observed at 24 h after injection ($p<0.05$).

At 48 h after injection, PFA perfused brains were extracted and the density of soluble Aβ40 in the brain was determined. An almost significant decrease of Aβ40 was observed in the treated group. As expected, the control wildtype mice did not show any detectable Aβ40 or Aβ42 in the plasma, nor detectable concentrations of Aβ40 in the brain (data not shown).

4. DISCUSSION

Aβ aggregation is considered to be directly involved in AD pathogenesis [42] and therefore inhibiting Aβ generation is of therapeutic interest.

In the present study, an immune VHH library for BACE1 affinity binders was successfully constructed. From this library, 28 phages were selected via phage display. A VHH ELISA identified 12 putative VHH candidates that bind to BACE1. Sequence analysis showed that these 12 VHHs represented three unique VHH sequences. This pool of three unique sequences is rather small for phage display selection, although, with selective elution, a lower number of unique sequences is generally found compared to panning selection and general elution using pH-shock. Selective elution was performed to enhance the discovery of inhibitory VHHs. Unexpectedly, the analysis of BACE1 activity modulation provided not only one inhibitory VHH (VHH-B3a), but also two stimulatory VHHs (VHH-B1a and -B5a).

The selected VHH-B3a consistently inhibited BACE1 activity in the biochemical and cellular assays, with only slight quantitative differences between the assays. Because the local available concentration of BACE1 in the cellular assay is unknown, the quantitative slope can vary from the biochemical slope. Although the most robust data are from biochemical assays, the cellular assay supports the biochemical data. By contrast, VHH-B1a functions inconsistently between the two assays, where the stimulation of BACE1 activity by VHH-B1a is clearly not as potent in the cellular assay compared to the stimulation of activity of purified BACE1 *in vitro*. This may be a result of the epitope that is targeted by VHH-B1a and the availability of this epitope for plasma membrane bound BACE1 [38]. By contrast, VHH-B3a shows a dose-dependent inhibition of BACE1 *in vitro* with a lower affinity compared to Inhibitor-IV, a known inhibitor of BACE1. A reduced activity of BACE1, rather than a complete inhibition, might be the preferred strategy for therapy, because a reduced Aβ40 and Aβ42 concentration already results in positive effects on AD symptoms [16,43–45]. Cross-breeding specific mice (BACE +/-) shows that a 50% reduction of BACE1 already has significant effects on AD pathology [43,44]. Full inhibition of BACE1 is most likely undesirable because a minimal concentration of Aβ might be crucial for cell survival [46]. However, the positive effects of a partially reduced BACE1 concentration do diminish with age and AD progression as a result of progressed pathology [22,47,48]. Nonetheless, for treatment of early AD patients and long-term treatment, it is significant not to diminish potential Aβ positive effects.

The *in vitro* finding of BACE1 inhibition was further evaluated *in vivo* by injecting IRD800 labelled VHH directly into the *cisterna magna* of APP_{swe}/PS1dE9 double transgenic mice. Random conjugation of a fluorophore to lysines may reduce the affinity of the VHH [49]. However, despite the presence of a lysine residue in the CDR3 of VHH-B3a, its activity is only slightly

reduced with random conjugation compared to non-conjugated VHH. Consequently, we could utilize the random conjugated VHH for *in vivo* application and evaluate its potential therapeutic effect.

First, distribution of the injected VHH in the brain was determined in wildtype mice. Next, transgenic mice at an age before the onset of Aβ plaque formation were injected with VHH-B3a-IRD800. Brain distribution showed that, with intracisternal injection, the VHH was distributed over the brain and resident for at least 24 h. The 24 h retention provided a sufficient time frame to evaluate Aβ concentration in plasma samples. Blood sampling of the mice treated with VHH-B3a-IRD800 showed a lowered concentration of Aβ40 and Aβ42 in plasma. Furthermore, a lowered density of soluble Aβ40 in the brain was measured.

The inhibition of BACE1 activity can be achieved by modulation of the active site of BACE1 or by allosteric inhibition [50]. By using a peptide containing the cleaving target of BACE1 for selective elution, we aimed to find VHH binding near or at the active site of BACE1. VHH could possibly bind to or near the flap region that covers the active site and modulate activity [51]. However, the stimulation of BACE1 activity is more unexpected because changing the active site of a protease normally results in decreased activity. A stimulatory effect of antibodies on BACE1 activity has been reported by Zhou *et al.* [52]. The authors describe how the tested antibodies (full length murine IgGs) bind unique structural loops on BACE1. The structural loops are identified as regulatory elements for BACE1 activity, yet are outside the active site of the enzyme [52]. It is possible that by capturing the peptide in our phage display set-up, the conformation of these structural loops is altered and VHHs that bind outside the BACE1 active site are eluted. Because co-crystallization of BACE1 with an inhibitor is possible [53], co-crystallization of BACE1 with VHH-B1a and -B3a might provide insight in the manner by which these VHHs modulate BACE1 activity.

Furthermore, the exact mechanism and relevance by which VHH-B3a lowers plasma Aβ concentrations remains to be fully determined. A chronic treatment of young transgenic mice before plaque formation may provide more information about the possibility for inhibiting plaque formation and neurodegeneration. Subsequently, chronic treatment of these mice after onset of AD pathology will determine the potential for inhibiting the progression of pathogenesis. In addition to mono treatment, combination treatment to target BACE1 as well as Aβ, can be considered using anti-Aβ antibodies or anti-Aβ VHH to improve overall efficacy in treatment [54].

Several strategies for BACE1 activity inhibition have already been explored and found to be useful. Next to small molecule inhibitors, antibodies have been raised and characterized to inhibit BACE1 activity. Inhibition of secretases with antibodies is successful in a number of diseases

[55–57] and antibodies are available to inhibit BACE1 activity [27,28]. Despite the availability of functional antibodies, we consider that VHH offer multiple benefits over conventional full length antibodies, provided that the selected VHHs bind specifically and with high affinity [58]. Several intrinsic characteristics make VHHs extremely qualified for inhibiting secretase activity compared to conventional antibodies. First of all, VHHs are equipped with a long protruding CDR3 loop that is suitable for inserting into cavities on the surface of the antigen [30,59]. Inhibition of lysozyme is an example in which this protruding loop is inserted into the active site of the enzyme [59]. Furthermore, VHHs have a very low immunogenic potential as a result of great homology with human VH domains, as well as the lack of an Fc-domain [30], and can be further humanized with relative ease [60]. These characteristics make VHHs very interesting for targeting and inhibiting secretase activity.

In the present study we deliberately circumvented the problem of brain delivery of VHHs by direct intracisternal injection. Circulation of VHHs upon systemic injection gives rise to additional problems such as rapid renal clearance and limited BBB passage. Solutions to minimize size-dependent renal clearance, while the molecule remains relatively small, are known for VHHs. An example is the noncovalent binding of serum albumin to temporarily increase size and serum retention [61,62]. Besides clearance, the protective function of the BBB obstructs the brain delivery of VHHs. However, BBB passage has been shown for specific VHHs. VHHs can cross the BBB both specifically for a certain VHH [34,63] and non-specifically for VHHs with a high isoelectric point (*i.e.* pI > 9.4) [64]. Because VHH-B3a does not comply with either criterion, other solutions need to be examined. VHH transport over the BBB via receptor-mediated transcytosis [65] or liposomes [66] are methods that have demonstrated the delivery of VHH into the brain.

5. CONCLUSION

Despite the remaining challenges, the present study shows that VHHs inhibiting BACE1 activity leading to lowered Aβ production can be selected from a llama immunized with recombinant BACE1. This finding provides optimism with respect to the generation of VHH-based therapeutics for the treatment of AD in the future.

DISCLOSURE

CTV and MEK are employees and shareholders of QVQ Holding BV, a biotechnology company developing single domain antibodies from camelids. BD, MR, ES, LW, SM, CTV, and MEK planned the experiments. BD, MR, DF, RS, ES, and MEK performed the experiments. BD, MR,

DF, RS, and MEK analysed data. LW, SM, and CTV contributed essential material. BD, MR, LW, SM, CTV, and MEK wrote and revised the published manuscript.

ACKNOWLEDGMENTS

The authors would like to thank Ivo Que of the Department of Endocrinology, LUMC, for acquiring the *in vivo* images of transgenic mice. The present study was supported financially by Agentschap NL (IOP IGE5005) and the Center for Medical Systems Biology (grants S-MRI-110010 and S-MRI-110030).

REFERENCES

1. Fargo, K. & Bleiler, L. Alzheimer's Association Report. 2014 Alzheimer's disease facts and figures. *Alzheimers Dement* 10(2):e47–92 (2014).
2. Glenner, G. G. & Wong, C. W. Alzheimer's disease: initial report of the purification and characterization of a novel cerebrovascular amyloid protein. *Biochem. Biophys. Res. Commun.* 120(3):885–890 (1984).
3. Tanzi, R. E. & Bertram, L. Twenty years of the Alzheimer's disease amyloid hypothesis: A genetic perspective. Cell 120(4):545–555 (2005).
4. Selkoe, D. J. Cell biology of the amyloid beta-protein precursor and the mechanism of Alzheimer's disease. *Annu. Rev. Cell Biol.* 10:373–403 (1994).
5. Han, W., Ji, T., Mei, B. & Su, J. Peptide p3 may play a neuroprotective role in the brain. *Med. Hypotheses* 76(4):543–546 (2011).
6. Hussain, I., Powell, D., Howlett, D. R., Tew, D. G., Meek, T. D., Chapman, C., Gloger, I. S., Murphy, K. E., Southan, C. D., Ryan, D. M., *et al.* Identification of a novel aspartic protease (Asp 2) as beta-secretase. *Mol. Cell. Neurosci.* 14(6):419–427 (1999).
7. Lin, X., Koelsch, G., Wu, S., Downs, D., Dashti, a & Tang, J. Human aspartic protease memapsin 2 cleaves the beta-secretase site of beta-amyloid precursor protein. *Proc. Natl. Acad. Sci. U. S. A.* 97(4):1456–1460 (2000).
8. Bodendorf, U., Fischer, F., Bodian, D., Multhaup, G. & Paganetti, P. A Splice Variant of Beta-Secretase Deficient in the Amyloidogenic Processing of the Amyloid Precursor Protein. *J. Biol. Chem.* 276(15):12019–12023 (2001).
9. Vassar, R., Bennett, B. D., Babu-Khan, S., Kahn, S., Mendiaz, E. a, Denis, P., Teplow, D. B., Ross, S., Amarante, P., Loeloff, R., *et al.* Beta-secretase cleavage of Alzheimer's amyloid precursor protein by the transmembrane aspartic protease BACE. *Science* 286(5440):735–741 (1999).
10. Sinha, S., Anderson, J. P., Barbour, R., Basi, G. S., Caccavello, R., Davis, D., Doan, M., Dovey, H. F., Frigon, N., Hong, J., *et al.* Purification and cloning of amyloid precursor protein beta-secretase from human brain. *Nature* 402(6761):537–540 (1999).
11. Yan, R., Bienkowski, M. J., Shuck, M. E., Miao, H., Tory, M. C., Pauley, a M., Brashier, J. R., Stratman, N. C., Mathews, W. R., Buhl, a E., *et al.* Membrane-anchored aspartyl protease with Alzheimer's disease beta-secretase activity. *Nature* 402(6761):533–537 (1999).
12. De Strooper, B. Aph-1, Pen-2, and Nicastrin with Presenilin generate an active gamma-Secretase complex. *Neuron* 38(1):9–12 (2003).
13. Fukumoto, H., Cheung, B. S., Hyman, B. T. & Irizarry, M. C. Beta-secretase protein and activity are increased in the neocortex in Alzheimer disease. *Arch. Neurol.* 59(9):1381–1389 (2002).
14. Ahmed, R. R., Holler, C. J., Webb, R. L., Li, F., Beckett, T. L. & Murphy, M. P. BACE1 and BACE2 enzymatic activities in Alzheimer's disease. *J. Neurochem.* 112(4):1045–1053 (2010).
15. Harada, H., Tamaoka, A., Ishii, K., Shoji, S., Kametaka, S., Kametani, F., Saito, Y. & Murayama, S. Beta-site APP cleaving enzyme 1 (BACE1) is increased in remaining neurons in Alzheimer's disease brains. *Neurosci. Res.* 54(1):24–29 (2006).
16. Laird, F. M., Cai, H., Savonenko, A. V, Farah, M. H., He, K., Melnikova, T., Wen, H., Chiang, H.-C., Xu, G., Koliatsos, V. E., *et al.* BACE1, a major determinant of selective vulnerability of the brain to amyloid-beta amyloidogenesis, is essential for cognitive, emotional, and synaptic functions. *J. Neurosci.* 25(50):11693–11709 (2005).
17. Cai, H., Wang, Y., McCarthy, D., Wen, H., Borchelt, D. R., Price, D. L. & Wong, P. C. BACE1 is the major beta-secretase for generation of Abeta peptides by neurons. *Nat. Neurosci.* 4(3):233–234 (2001).
18. Luo, Y., Bolon, B., Kahn, S., Bennett, B. D., Babu-Khan, S., Denis, P., Fan, W., Kha, H., Zhang, J., Gong, Y., *et al.* Mice deficient in BACE1, the Alzheimer's β-secretase, have normal phenotype and abolished β-amyloid generation. *Nat. Neurosci.* 4(3):231–232 (2001).

19. Roberds, S. L., Anderson, J., Basi, G., Bienkowski, M. J., Branstetter, D. G., Chen, K. S., Freedman, S. B., Frigon, N. L., Games, D., Hu, K., *et al.* BACE knockout mice are healthy despite lacking the primary beta-secretase activity in brain: implications for Alzheimer's disease therapeutics. *Hum. Mol. Genet.* 10(12):1317–1324 (2001).

20. Ohno, M., Sametsky, E. a., Younkin, L. H., Oakley, H., Younkin, S. G., Citron, M., Vassar, R. & Disterhoft, J. F. BACE1 Deficiency Rescues Memory Deficits and Cholinergic Dysfunction in a Mouse Model of Alzheimer's Disease. *Neuron* 41(1):27–33 (2004).

21. Sankaranarayanan, S., Holahan, M. a., Colussi, D., Crouthamel, M.-C., Devanarayan, V., Ellis, J., Espeseth, A., Gates, A. T., Graham, S. L., Gregro, A. R., *et al.* First demonstration of cerebrospinal fluid and plasma Aβ lowering with oral administration of a β-site amyloid precursor protein-cleaving enzyme 1 inhibitor in nonhuman primated. *J. Pharmacol. Exp. Ther.* 328(1):131–140 (2009).

22. Fukumoto, H., Takahashi, H., Tarui, N., Matsui, J., Tomita, T., Hirode, M., Sagayama, M., Maeda, R., Kawamoto, M., Hirai, K., *et al.* A noncompetitive BACE1 inhibitor TAK-070 ameliorates Abeta pathology and behavioral deficits in a mouse model of Alzheimer's disease. *J. Neurosci.* 30(33):11157–11166 (2010).

23. Mancini, F., De Simone, A. & Andrisano, V. Beta-secretase as a target for Alzheimer's disease drug discovery: An overview of *in vitro* methods for characterization of inhibitors. *Anal. Bioanal. Chem.* 400(7):1979–1996 (2011).

24. Cully, M. Deal watch: Lilly buys back into the BACE race for Alzheimer's disease. *Nat. Rev. Drug Discov.* 13(11):804–804 (2014).

25. Eketjall, S., Janson, J., Jeppsson, F., Svanhagen, a., Kolmodin, K., Gustavsson, S., Radesater, a.-C., Eliason, K., Briem, S., Appelkvist, P., *et al.* AZ-4217: A High Potency BACE Inhibitor Displaying Acute Central Efficacy in Different *In Vivo* Models and Reduced Amyloid Deposition in Tg2576 Mice. *J. Neurosci.* 33(24):10075–10084 (2013).

26. Vassar, R. BACE1 inhibitor drugs in clinical trials for Alzheimer's disease. *Alzheimers. Res. Ther.* 6(9):1–14 (2014).

27. Rakover, I., Arbel, M. & Solomon, B. Immunotherapy against APP beta-secretase cleavage site improves cognitive function and reduces neuroinflammation in Tg2576 mice without a significant effect on brain abeta levels. *Neurodegener. Dis.* 4(5):392–402 (2007).

28. Arbel, M. & Solomon, B. A Novel Immunotherapy for Alzheimers Disease: Antibodies against the Beta-Secretase Cleavage Site of APP. *Curr. Alzheimer Res.* 4(4):437–445 (2007).

29. Chang, W.-P., Downs, D., Huang, X.-P., Da, H., Fung, K.-M. & Tang, J. Amyloid-beta reduction by memapsin 2 (beta-secretase) immunization. *FASEB J.* 21(12):3184–3196 (2007).

30. Muyldermans, S. Nanobodies: natural single-domain antibodies. *Annu. Rev. Biochem.* 82(1):775–797 (2013).

31. Hamers-Casterman, C., Atarhouch, T., Muyldermans, S., Robinson, G., Hamers, C., Songa, E. B., Bendahman, N. & Hamers, R. Naturally occurring antibodies devoid of light chains. *Nature* 363(6428):446–448 (1993).

32. Dumoulin, M., Last, A. M., Desmyter, A., Decanniere, K., Canet, D., Larsson, G., Spencer, A., Archer, D. B., Sasse, J., Muyldermans, S., *et al.* A camelid antibody fragment inhibits the formation of amyloid fibrils by human lysozyme. *Nature* 424(6950):783–788 (2003).

33. Desmyter, A., Spinelli, S., Payan, F., Lauwereys, M., Wyns, L., Muyldermans, S. & Cambillau, C. Three camelid VHH domains in complex with porcine pancreatic alpha-amylase: Inhibition and versatility of binding topology. *J. Biol. Chem.* 277(26):23645–23650 (2002).

34. Muruganandam, A., Tanha, J., Narang, S. & Stanimirovic, D. Selection of phage-displayed llama single-domain antibodies that transmigrate across human blood-brain barrier endothelium. *FASEB J.* 16(2):240–2 (2002).

35. Thinakaran, G., Teplow, D. B., Siman, R., Greenberg, B. & Sisodiat, S. S. Metabolism of the 'Swedish' amyloid precursor protein variant in neuro2a (N2a) cells: Evidence that cleavage at the 'beta-secretase' site occurs in the Golgi apparatus. *J. Biol. Chem.* 271(16):9390–9397 (1996).

36. Verheesen, P., Roussis, A., de Haard, H. J., Groot, A. J., Stam, J. C., den Dunnen, J. T., Frants, R. R., Verkleij, A. J., Theo Verrips, C. & van der Maarel, S. M. Reliable and controllable antibody fragment selections from Camelid non-immune libraries for target validation. *Biochim. Biophys. Acta* 1764(8):1307–19 (2006).

37. Hoogenboom, H. R., de Bruïne, A. P., Hufton, S. E., Hoet, R. M., Arends, J. W. & Roovers, R. C. Antibody phage display technology and its applications. *Immunotechnology* 4(1):1–20 (1998).

38. Stockley, J. H. & O'Neill, C. Understanding BACE1: Essential protease for amyloid-beta production in Alzheimer's disease. *Cell. Mol. Life Sci.* 65(20):3265–3289 (2008).

39. Mandell, J. G., Neuberger, T., Drapaca, C. S., Webb, A. G. & Schiff, S. J. The dynamics of brain and cerebrospinal fluid growth in normal versus hydrocephalic mice. *J. Neurosurg. Pediatr.* 6(1):1–10 (2010).

40. Vanderstichele, H., Van Kerschaver, E., Hesse, C., Davidsson, P., Buyse, M. A., Andreasen, N., Minthon, L., Wallin, A., Blennow, K. & Vanmechelen, E. Standardization of measurement of beta-amyloid(1-42) in cerebrospinal fluid and plasma. *Amyloid* 7(4):245–58 (2000).

41. Hansson, O., Zetterberg, H., Vanmechelen, E., Vanderstichele, H., Andreasson, U., Londos, E., Wallin, A., Minthon, L. & Blennow, K. Evaluation of plasma ABeta40 and ABeta42 as predictors of conversion to Alzheimer's disease in patients with mild cognitive impairment. *Neurobiol. Aging* 31(3):357–367 (2010).

42. Selkoe, D. J. Alzheimer's disease: genes, proteins, and therapy. *Physiol. Rev.* 81(2):741–766 (2001).

43. McConlogue, L., Buttini, M., Anderson, J. P., Brigham, E. F., Chen, K. S., Freedman, S. B., Games, D., Johnson-Wood, K., Lee, M., Zeller, M., *et al.* Partial reduction of BACE1 has dramatic effects on Alzheimer plaque and synaptic pathology in APP transgenic mice. *J. Biol. Chem.* 282(36):26326–26334 (2007).

44. Kimura, R., Devi, L. & Ohno, M. Partial reduction of BACE1 improves synaptic plasticity, recent and remote memories in Alzheimer's disease transgenic mice. *J. Neurochem.* 113(1):248–261 (2010).

45. Chabrier, M. A., Blurton-Jones, M., Agazaryan, A. A., Nerhus, J. L., Martinez-Coria, H. & LaFerla, F. M. Soluble aβ promotes wild-type tau pathology *in vivo*. *J. Neurosci.* 32(48):17345–50 (2012).

46. Plant, L. D., Boyle, J. P., Smith, I. F., Peers, C. & Pearson, H. a. The production of amyloid beta peptide is a critical requirement for the viability of central neurons. *J. Neurosci.* 23(13):5531–5535 (2003).

47. Chang, W.-P., Huang, X., Downs, D., Cirrito, J. R., Koelsch, G., Holtzman, D. M., Ghosh, A. K. & Tang, J. Beta-secretase inhibitor GRL-8234 rescues age-related cognitive decline in APP transgenic mice. *FASEB J.* 25(2):775–784 (2011).

48. Devi, L. & Ohno, M. Mechanisms that lessen benefits of β-secretase reduction in a mouse model of Alzheimer's disease. *Transl. Psychiatry* 3(7):e284 (2013).

49. Kijanka, M., Warnders, F. J., El Khattabi, M., Lub-De Hooge, M., Van Dam, G. M., Ntziachristos, V., De Vries, L., Oliveira, S. & Van Bergen En Henegouwen, P. M. P. Rapid optical imaging of human breast tumour xenografts using anti-HER2 VHHs site-directly conjugated to IRDye 800CW for image-guided surgery. *Eur. J. Nucl. Med. Mol. Imaging* 40(11):1718–1729 (2013).

50. Wang, W., Liu, Y. & Lazarus, R. a. Allosteric inhibition of BACE1 by an exosite-binding antibody. *Curr. Opin. Struct. Biol.* 23(6):797–805 (2013).

51. Davies, D. R. The structure and function of the aspartic proteinases. *Annu. Rev. Biophys. Biophys. Chem.* 19:189–215 (1990).

52. Zhou, L., Chávez-Gutiérrez, L., Bockstael, K., Sannerud, R., Annaert, W., May, P. C., Karran, E. & De Strooper, B. Inhibition of β-secretase *in vivo* via antibody binding to unique loops (D and F) of BACE1. *J. Biol. Chem.* 286(10):8677–8687 (2011).

53. Durham, T. B. & Shepherd, T. A. Progress toward the discovery and development of efficacious BACE inhibitors. *Curr. Opin. Drug Discov. Devel.* 9(6):776–91 (2006).

54. Jacobsen, H., Ozmen, L., Caruso, a., Narquizian, R., Hilpert, H., Jacobsen, B., Terwel, D., Tanghe, a. & Bohrmann, B. Combined Treatment with a BACE Inhibitor and Anti-A Antibody Gantenerumab Enhances Amyloid Reduction in APPLondon Mice. *J. Neurosci.* 34(35):11621–11630 (2014).

55. Hayashi, I., Takatori, S., Urano, Y., Iwanari, H., Isoo, N., Osawa, S., Fukuda, M. a., Kodama, T., Hamakubo, T., Li, T., *et al.* Single chain variable fragment against nicastrin inhibits the γ-secretase activity. *J. Biol. Chem.* 284(41):27838–27847 (2009).

56. Fong, J. E., Le Nihouannen, D. & Komarova, S. V. Tumor-supportive and osteoclastogenic changes induced by breast cancer-derived factors are reversed by inhibition of γ-secretase. *J. Biol. Chem.* 285(41):31427–31434 (2010).

57. Huang, H. S., Buck, C. B. & Lambert, P. F. Inhibition of gamma secretase blocks HPV infection. *Virology* 407(2):391–396 (2010).

58. Van Bockstaele, F., Holz, J.-B. & Revets, H. The development of nanobodies for therapeutic applications. *Curr. Opin. Investig. Drugs* 10(11):1212–24 (2009).

59. Desmyter, A., Transue, T. R., Ghahroudi, M. A., Thi, M. H., Poortmans, F., Hamers, R., Muyldermans, S. & Wyns, L. Crystal structure of a camel single-domain VH antibody fragment in complex with lysozyme. *Nat. Struct. Biol.* 3(9):803–811 (1996).

60. Vincke, C., Loris, R., Saerens, D., Martinez-Rodriguez, S., Muyldermans, S. & Conrath, K. General strategy to humanize a camelid single-domain antibody and identification of a universal humanized nanobody scaffold. *J. Biol. Chem.* 284(5):3273–84 (2009).

61. Roovers, R. C., Laeremans, T., Huang, L., De Taeye, S., Verkleij, A. J., Revets, H., De Haard, H. J. & Van Bergen En Henegouwen, P. M. P. Efficient inhibition of EGFR signalling and of tumour growth by antagonistic anti-EGFR Nanobodies. *Cancer Immunol. Immunother.* 56(3):303–317 (2007).

62. Harmsen, M. M. & De Haard, H. J. Properties, production, and applications of camelid single-domain antibody fragments. *Appl. Microbiol. Biotechnol.* 77(1):13–22 (2007).

63. Rutgers, K. S., Nabuurs, R. J. A., van den Berg, S. A. A., Schenk, G. J., Rotman, M., Verrips, C. T., van Duinen, S. G., Maat-Schieman, M. L., van Buchem, M. A., de Boer, A. G., *et al.* Transmigration of beta amyloid specific heavy chain antibody fragments across the *in vitro* blood-brain barrier. *Neuroscience* 190:37–42 (2011).

64. Li, T., Bourgeois, J.-P., Celli, S., Glacial, F., Le Sourd, A.-M., Mecheri, S., Weksler, B., Romero, I., Couraud, P.-O., Rougeon, F., *et al.* Cell-penetrating anti-GFAP VHH and corresponding fluorescent fusion protein VHH-GFP spontaneously cross the blood-brain barrier and specifically recognize astrocytes: application to brain imaging. *FASEB J.* 26(10):3969–79 (2012).

65. Yu, Y. J., Atwal, J. K., Zhang, Y., Tong, R. K., Wildsmith, K. R., Tan, C., Bien-Ly, N., Hersom, M., Maloney, J. A., Meilandt, W. J., *et al.* Therapeutic bispecific antibodies cross the blood-brain barrier in nonhuman primates. *Sci. Transl. Med.* 6(261):261ra154 (2014).

66. Rotman, M., Welling, M. M., Bunschoten, A., de Backer, M. E., Rip, J., Nabuurs, R. J. A., Gaillard, P. J., van Buchem, M., van der Maarel, S. M. & van der Weerd, L. Enhanced liposomal brain delivery of an anti-amyloid VHH-2H heavy chain antibody fragment in a mouse model for Alzheimer's disease. *J. Control. Release* 203:40–50 (2015).

* Authors contributed equally to this work.
1. Department of Human Genetics, Leiden University Medical Center, The Netherlands
2. Department of Radiology, Leiden University Medical Center, The Netherlands
3. to-BBB technologies BV, Leiden, The Netherlands